JGR Atmospheres

RESEARCH ARTICLE
10.1029/2020JD033459

Model and Satellite Analysis of Transport of Asian Anthropogenic Pollution to the Arctic: Siberian and Pacific Pathways and Their Meteorological Controls

Kohei Ikeda[1], Hiroshi Tanimoto[1], Takafumi Sugita[1], Hideharu Akiyoshi[1], Cathy Clerbaux[2,3], and Pierre-François Coheur[3]

[1]Center for Global Environmental Research, National Institute for Environmental Studies, Tsukuba, Ibaraki, Japan, [2]LATMOS/IPSL, Sorbonne Université, UVSQ, CNRS, Paris, France, [3]Université libre de Bruxelles (ULB), Service de Chimie Quantique et Photophysique, Atmospheric Spectroscopy, Brussels, Belgium

Key Points:

- Eleven events of anthropogenic black carbon from East Asia to the Arctic were identified by an integrated satellite and model analysis
- Two transport patterns from East Asia were identified; Siberia and the North Pacific en route to the Arctic
- Low pressures passing through Siberia and high pressures staying around the Bering Sea had key roles in Siberian and Pacific route events

Supporting Information:

Supporting Information may be found in the online version of this article.

Correspondence to:

K. Ikeda and H. Tanimoto,
ikeda.kohei@nies.go.jp;
tanimoto@nies.go.jp

Citation:

Ikeda, K., Tanimoto, H., Sugita, T., Akiyoshi, H., Clerbaux, C., & Coheur, P.-F. (2021). Model and satellite analysis of transport of Asian anthropogenic pollution to the Arctic: Siberian and Pacific pathways and their meteorological controls. *Journal of Geophysical Research: Atmospheres*, *126*, e2020JD033459. https://doi.org/10.1029/2020JD033459

Received 6 JUL 2020
Accepted 14 MAR 2021

Abstract We made comprehensive analyses of long-range transport episodes of air pollutants from East Asia to the Arctic and associated meteorological conditions. While our main focus was black carbon (BC) as its transport to the Arctic has attracted great attention, carbon monoxide (CO) was also diagnosed as a species co-emitted with BC and as a tracer of long-range transport. We used satellite observations by the Infrared Atmospheric Sounding Interferometer (IASI) and a newly implemented BC tagged-tracer simulation using a global chemical transport model, GEOS-Chem. Temporal variations of IASI-CO column over the Pacific Arctic (160–200°E, 60–80°N) showed that episodic increases occurred several times in each season. For the period of 2007–2011, 11 strong events (6 in spring, 3 in autumn, and 2 in winter) caused by the long-range transport from East Asia were identified. Two transport pathways from East Asia to the Arctic were found: over Siberia and the Sea of Okhotsk, and over the North Pacific. In the pathway over Siberia and the Sea of Okhotsk, the pollutants were transported northeastward from China mainly through the Sea of Okhotsk and East Siberia. The low pressures passing from East Siberia to the Sea of Okhotsk played important roles in the transport in the lower troposphere and uplifting to the middle troposphere. In the pathway over the North Pacific, the pollutants were transported eastward from the Asian continent and subsequent northward transport took place over the North Pacific. The poleward transport occurred west of the high pressure that stayed around the Bering Sea.

Plain Language Summary Arctic air pollution that includes aerosols and tropospheric ozone has great impacts on the climate and environment in the Arctic. However, there are still large uncertainties in the quantification of its influences on climate change, human health, and the ecosystem in the Arctic. Black carbon (BC) is a key air pollutant because it can contribute to the Arctic warming by absorbing solar radiation in the atmosphere and by reducing snow and ice albedo due to deposition on these surfaces. In the present study, we made comprehensive analyses of long-range transport episodes of BC and carbon monoxide from East Asia to the Arctic and associated meteorological conditions. Eleven events caused by the long-range transport from East Asia were identified. Two transport pathways from East Asia to the Arctic were found: over Siberia and the Sea of Okhotsk, and over the North Pacific. The findings on the transport pathways and the associated meteorological conditions can provide valuable knowledge for the planning of field campaigns and can be used as the characteristics of long-range transport from East Asia to the Arctic under the current climate to examine the impact of the future climate on the transport from Asia to the Arctic.

1. Introduction

Arctic air pollution that includes short-lived climate pollutants such as aerosols and tropospheric ozone has great impacts on the climate and environment in the Arctic (Quinn et al., 2008; Sand et al., 2016; Shindell, 2007). However, there are still large uncertainties in the quantification of its influences on climate change, human health, and the ecosystem in the Arctic (Arnold et al., 2016). Black carbon (BC) is a key air pollutant because it has positive radiative forcing in the Arctic by absorbing solar radiation in the atmosphere and by reducing snow and ice albedo due to deposition on these surfaces (AMAP, 2015; Flanner et al., 2007; Quinn et al., 2007). However, model inter-comparison studies showed difficulties and large

diversities in reproducing observed seasonal variations, concentration levels, and vertical profiles of BC over the Arctic (Eckhardt et al., 2015; Lee et al., 2013). They are caused by uncertainties in the model treatments of transformation from hydrophobic to hydrophilic BC and wet removal processes during long-range transport from source regions to the Arctic (Bourgeois & Bey, 2011; Liu et al., 2011). Additionally, these discrepancies highlight the need to improve the understanding of long-range transport of air pollutants because major sources of the Arctic air pollutants are emissions from the northern middle and high latitudes: Europe, Russia, East Asia, and North America (Hirdman et al., 2010; Ikeda et al., 2017; Sharma et al., 2013; Shindell et al., 2008; Wang et al., 2011, 2014).

East Asia is the region with the largest emissions of anthropogenic air pollutants (Janssens-Maenhout et al., 2015) and thus the emissions from this region have great impacts on the global and regional climate and air quality including the Arctic (AMAP, 2015). To better assess the impact of East Asian BC on the Arctic climate and environment, it is important to improve model reproducibility by evaluating models using in-situ measurements such as aircraft observations (Lund et al., 2018). This indicates the necessity of an improved understanding of the transport pathways from East Asia to the Arctic and associated meteorological conditions on a daily timescale for future observations and model inter-comparison studies. Previous studies on exports of air pollutants from East Asia mainly focused on the uplifting processes from the boundary layer to the free troposphere and eastward transport to the North Pacific and North America (Clarisse et al., 2011; Cooper et al., 2004; Hadley et al., 2007; Liang et al., 2004; Luan & Jaeglé, 2013; Oshima et al., 2013). There are a few studies that investigated pollutant transport events reaching the Arctic from East Asia. For instance, Di Pierro et al. (2011) examined three events of long-range transport of aerosol from East Asia to the Arctic using CALIPSO observations and a chemical transport model, indicating the transport patterns over Siberia and meteorological conditions associated with these events. Matsui et al. (2011) investigated the pathways and efficiencies of BC transport from the Asian continent to the Arctic using data obtained by the ARCTAS (Arctic Research of the Composition of the Troposphere from Aircraft and Satellites) aircraft campaign and a chemical transport model.

Our previous study examined seasonally averaged transport patterns from various source regions including East Asia to the Arctic by tagged BC simulations using a global chemical transport model, GEOS-Chem (Ikeda et al., 2017). The model demonstrated that BC emitted from East Asia was transported to the Arctic mainly through the Sea of Okhotsk and eastern Siberia in the middle troposphere. We also identified an important region where a strong inflow from East Asia to the Arctic occurred (130–180°E and 3–8 km at 66°N) (Ikeda et al., 2017). In the present study, we analyzed long-range transport events of BC and carbon monoxide (CO) from East Asia to the Arctic using satellite measurements and a global chemical transport model GEOS-Chem. CO is commonly emitted with BC by fossil fuel combustion and biomass burning and is useful as a tracer of long-range transport of polluted plumes due to its relatively long lifetime of 1–2 months (e.g., Liang et al., 2004). The present study focused on episodic transport events from East Asia to the Arctic on a daily scale to elucidate transport mechanisms and synoptic-scale meteorological conditions. We examined 11 long-range transport events during 2007–2011 and found that they could be classified into two distinct transport patterns based on their pathways: The Siberia and the Sea of Okhotsk route (hereinafter referred to as the Siberian route) and the North Pacific route (hereinafter referred to as the Pacific route). In addition to the analysis of individual events, we performed a composite analysis to further clarify the key features of the transport pathways and the meteorological fields of both route events.

2. Observational and Model Data

We used CO data provided by the IASI (Infrared Atmosphere Sounding Interferometer) instrument (Clerbaux et al., 2009) onboard the Metop-A platform since October 2006. IASI measures thermal infrared spectra at a horizontal resolution of 50 km (4 simultaneous pixels of 12 km at nadir) with a swath width of about 2200 km. It crosses the equator at 9:30 and 21:30 solar local times and provides global monitoring of atmospheric composition twice a day. CO total column is retrieved by the Fast Optical Retrievals on Layers for IASI retrieval algorithm (George et al., 2009). We used the daily total CO column (v20100815) that includes observed data for 24 h of each day.

We performed tagged BC simulations using a global chemical transport model, GEOS-Chem version 9-02 (Bey et al., 2001; Ikeda et al., 2017) to examine the long-range transport from East Asia to the Arctic. The horizontal resolution was 2° × 2.5° with 47 vertical layers from the surface to 0.01 hPa. GEOS-Chem is driven by assimilated meteorological data from the Goddard Earth Observing System (GEOS-5) provided by the NASA Global Modeling and Assimilation Office. In the tagged tracer simulations, we distinguished the BC tracers by source type (i.e., anthropogenic and biomass burning) and region. The global domain was divided into 16 and 27 regions for anthropogenic and biomass burning emissions, respectively (see Figure S1 and Figure 1 of Ikeda et al., 2017). Here, East Asia was defined as the sum of Japan, the Korean Peninsula, North China, and South China. For anthropogenic emissions, we used the BC emissions of HTAP v2.2 (Janssens-Maenhout et al., 2015), which had been developed for the experiments of HTAP Phase 2. For biomass burning emissions, we adopted Global Fire Emissions Database v3.1 with 0.5° × 0.5° of spatial resolution and daily temporal resolution (van der Werf et al., 2010). We performed the tagged simulation for 5 years from 2007 to 2011 after a model spin-up of 6 months.

In our previous study, we modified the aging and wet removal processes of BC to improve model reproducibility over the Arctic (Ikeda et al., 2017). The aging parameterization of Liu et al. (2011), in which a timescale of BC aging is derived from the number concentration of OH radical, was implemented instead of using a constant aging time of 1.15 days in the standard GEOS-Chem. The monthly average OH distributions for the calculation of BC aging time were stored by the full-chemistry simulation of GEOS-Chem version v9-02. In GEOS-Chem, the wet scavenging process distinguishes between liquid and ice clouds for in-cloud scavenging (rainout) (Wang et al., 2011). The scavenging rate of hydrophobic BC by ice cloud ($T < 258$ K) was reduced to 5% of water-soluble aerosols for liquid clouds by following earlier studies (Bourgeois & Bey, 2011). Our previous study showed that the BC simulation with the modified schemes reproduced the seasonal variations observed at Arctic sites and the vertical profiles over the Arctic obtained by the ARCTAS campaign (Ikeda et al., 2017). More details of the model evaluation were described in Ikeda et al. (2017).

3. Results and Discussion

3.1. Long-Range Transport Events From East Asia to the Arctic

We examined long-range transport events from East Asia to the Arctic during 2007–2011 by analyzing satellite measurements and tagged tracer simulations to elucidate transport pathways, mechanisms, and meteorological conditions. First, we investigated the temporal variations of the daily CO column measured by IASI averaged over the Pacific Arctic (160–200°E; 60–80°N) to identify long-range transport events from East Asia to the Arctic (Figure 1). This region of interest was chosen as an entrance region from East Asia to the Arctic based on previous studies (Barrie, 1986; Di Pierro et al., 2011; Ikeda et al., 2017). Ikeda et al. (2017) identified an important region where a strong poleward flow from East Asia occurred (130–180°E and 3–8 km at 66°N), and showed that this place did not change in seasons. We confirmed that the temporal variations of the East Asian BC were similar when different longitude ranges including Siberia and North America (120–200°E, 160–240°E) were used for the region of interest (not shown). The mean concentrations of CO column were determined as a 30-days running average. They increased during spring and decreased in early autumn. In addition to the seasonal variation of the mean concentrations, the daily variations of the CO column showed that enhancements from a few days to a week were observed one or two times a month. We used ΔCO to identify an event, which was calculated by subtracting mean concentrations from the observed values. The events were defined as days when ΔCO exceeded 2.0×10^{17} molecules cm^{-2} to select the approximately top 10% of the enhancements above the mean concentrations. There were 116 events during 2007–2011, corresponding to 8% of the total observation days. The frequency of the events was highest (42 days) in spring (March–May) and lowest (18 days) in winter (December–February).

The simulated BC column averaged over the same area (160–200°E; 60–80°N) also showed enhancement during the periods when the IASI CO column increased (Figure 1). Comparing the total BC and East Asian BC, it is suggested that most events except those during summer were caused by long-range transport from East Asia. Over the Pacific Arctic, the contribution from East Asian BC was predominant compared to other anthropogenic sources in northern mid-high latitudes such as Europe, Russia, and Northern America (see Figure S2). East Asian BC did not increase during the events in summer because the transport from East Asia to the Arctic is weak in this season (Ikeda et al., 2017). The main sources of enhancements during

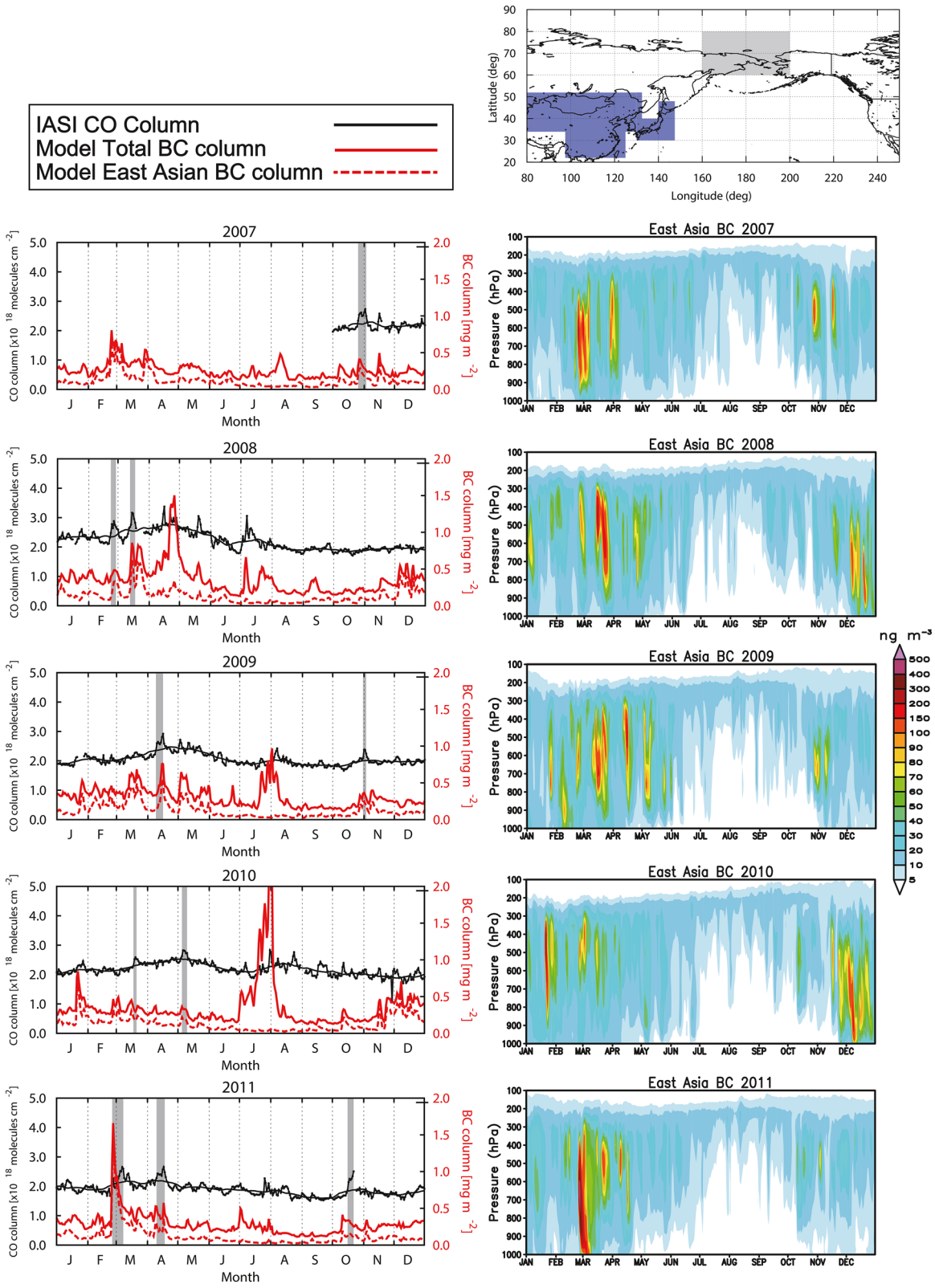

Figure 1. Left column: Observed CO column (solid black line for daily average and thin black line for 30-days running average) and simulated BC column (solid red line for total BC and dotted red line for East Asian BC) averaged over the Pacific side of the Arctic (160–200°E and 60–80°N) during 2007–2011. The gray shade indicates 11 transport events from East Asia. Right column: Daily altitude cross sections of East Asian BC averaged over the research area. The map shows the research area of the average (gray) and the East Asian domain (blue).

Table 1
Long-Range Transport Events From East Asia to the Arctic in 2007–2011

Date	Transport pathway	Transport time (days)	Duration (days)	IASI CO column (molecules cm^{-2})[a]	Model east asian BC column (mg m^{-2})[b]
October 27–November 3, 2007	Siberia	4	8	$3.4 \times 10^{17} \pm 0.75 \times 10^{17}$	0.22 ± 0.044
February 24–February 28, 2008	Pacific	6	5	$3.8 \times 10^{17} \pm 0.88 \times 10^{17}$	0.28 ± 0.062
March 14–March 18, 2008	Siberia	4	5	$4.3 \times 10^{17} \pm 1.7 \times 10^{17}$	0.44 ± 0.13
April 10–April 16, 2009	Siberia	5	7	$3.2 \times 10^{17} \pm 1.1 \times 10^{17}$	0.32 ± 0.15
November 1–November 3, 2009	Pacific	6	3	$3.2 \times 10^{17} \pm 0.61 \times 10^{17}$	0.22 ± 0.023
March 19–March 21, 2010	Pacific	6	3	$2.4 \times 10^{17} \pm 0.29 \times 10^{17}$	0.19 ± 0.010
May 6–May 10, 2010	Pacific	7	5	$2.6 \times 10^{17} \pm 0.42 \times 10^{17}$	0.19 ± 0.018
February 26–February 28, 2011	Siberia	5	3	$2.1 \times 10^{17} \pm 1.6 \times 10^{17}$	1.2 ± 0.22
March 1–March 8, 2011	Pacific	5	8	$3.9 \times 10^{17} \pm 0.94 \times 10^{17}$	0.43 ± 0.072
April 11–April 18, 2011	Siberia	5	8	$3.0 \times 10^{17} \pm 0.94 \times 10^{17}$	0.22 ± 0.060
October 17–October 22, 2011	Siberia	4	6	$4.3 \times 10^{17} \pm 1.1 \times 10^{17}$	0.14 ± 0.020

[a]Average and standard deviation of the enhancement of the IASI CO column for the event duration. [b]Average and standard deviation of the model East Asian BC column for the event duration.

summer were probably biomass burning emissions from boreal forests in Siberia and Northern America (Stohl et al., 2006). In April 2008, while the total BC was enhanced, the East Asian BC showed a modest increase. Matsui et al. (2011) reported that the biomass burning emissions in Russia were the most important sources of BC transported to the Pacific Arctic in April 2008. In this study, major events from East Asia were defined by the following conditions: (1) ΔCO averaged over the Pacific Arctic exceeded 2.0×10^{17} molecules cm^{-2} for at least 3 days; (2) simulated BC was enhanced from the monthly averages and the relative contribution of the East Asian BC to the total BC was higher than 50%. As a result, 11 events from East Asia to the Arctic were identified during 2007–2011, which occurred six times in spring, three times in autumn, and two times in winter (Table 1, Figure 1).

Figure 1 also shows the time-altitude distributions of the daily concentrations of East Asian BC. The increases of the East Asian BC during the transport events were seen mainly at 300–800 hPa with a maximum around 500 hPa. This result indicates that the transport from East Asia to the Arctic occurred mainly in the middle troposphere, and inflow in the lower troposphere was basically weak (Di Pierro et al., 2011; Ikeda et al., 2017; Klonecki et al., 2003; Stohl, 2006). However, the model demonstrated that there were a few events in which the East Asian BC was enhanced in the lower troposphere including near the surface (e.g., March 2011) as described in detail below.

We firstly examined the transport patterns and meteorological conditions in the lower and middle troposphere for each of the 11 events that occurred during 2007–2011 on a daily scale. Based on tracking the plumes of East Asian pollutants, we classified the events into two transport routes and mechanisms: The Siberian route and the Pacific route. For the Siberian route, pollutants were transported from China to the Arctic Ocean mainly over the Sea of Okhotsk and East Siberia. For the Pacific route, East Asian BC was transported eastward from the Asian continent to the Northwest Pacific, and subsequent poleward transport occurred over the North Pacific and the Bering Sea. As a result of the analysis of the 11 cases, six events were classified as the Siberian route and the other five cases corresponded to the Pacific route (Table 1).

The enhancement of the CO column (ΔCO) over the Pacific Arctic (160–180°E, 60–80°N) measured by IASI during each event was 2.1×10^{17}–4.3×10^{17} molecules cm^{-2} for the Siberian route and 2.4×10^{17}–3.9×10^{17} molecules cm^{-2} for the Pacific route (Table 1). The averaged value of the six events of the Siberian route (3.5×10^{17} molecules cm^{-2}) was similar to that of the Pacific route events (3.3×10^{17} molecules cm^{-2}). The column of East Asian BC over the Pacific Arctic was estimated to be 0.14–1.2 mg m^{-2} for the Siberian route and 0.19–0.43 mg m^{-2} for the Pacific route (Table 1). The averaged East Asian BC column of the Siberian route (0.28 mg m^{-2}) was also similar to that of the Pacific route (0.27 mg m^{-2}).

3.2. Siberian Route Event

For a case study of the Siberian route, we examined the transport pattern and associated meteorological conditions of a pollution event that occurred in October 2007. We chose this event as a typical case among six events of the Siberian route (see Figure S3). Figure 2 shows the daily horizontal distributions of East Asian BC concentrations, horizontal winds, and geopotential height at 850 and 500 hPa. In addition to the transport patterns in the lower and middle troposphere, sea level pressure and precipitation are also shown in Figure 2. At an early stage of the event (24–26 October), the East Asian BC spread northeastward from North China to the Sea of Okhotsk in the lower troposphere. This transport was caused by southwesterly winds blowing south of a low pressure that had generated around the border between China and Russia (120°E, 55°N) on 24 October. This cyclone moved northeastward to the Sea of Okhotsk through East Siberia until 27 October. The surface track of this low pressure was located at a relatively high latitude in the cyclones over East Asia (Chen et al., 1991). The cyclones passing through a similar route played an important role in other events of the Siberian route as described below. The horizontal distribution of East Asian BC at 500 hPa showed that upward transport to the middle troposphere occurred around 140°E and 55°N over East Siberia on 25 October (Figure 2). The uplifting occurred south of the low-pressure center, suggesting that the plume was transported upward by the warm conveyer belt (Cooper et al., 2004).

At 500 hPa, the plume of the East Asian BC was transported northeastward over East Siberia and reached the Arctic two days after the upward transport to the free troposphere. The geopotential height at 500 hPa showed that the East Asian BC was transported to the Arctic by southwesterly winds blowing between the trough and ridge. Because this disturbance moved northeastward over East Siberia, the plume of the East Asian BC between the trough and ridge reached the Arctic. After arriving at the Arctic, it was further transported eastward over the Arctic Ocean. It took about five days for the plume to be transported from East Asia to the Arctic. We found that a low-pressure system passing through from East Siberia to the Sea of Okhotsk played an important role in the long-range transport of the Siberian route event.

3.3. Pacific Route Event

Next, we examined a Pacific route event that occurred in February–March 2011. This event showed the largest enhancement of the IASI CO column among five events of the Pacific route (Table 1) and an increase in BC was also observed at the Arctic site of Barrow as shown below. Figure 3 shows the horizontal distributions of East Asian BC and meteorological fields for February 26–March 2, 2011. At 500 hPa, a plume of East Asian BC was transported eastward from North China (125°E, 45°N) to the central North Pacific (180°E, 35°N) by westerly winds on 26–28 February. The upward transport and outflow from the Asian continent were caused by a low pressure over North China (115°E, 45°N). After the eastward transport to the central North Pacific, East Asian BC was transported northward over the North Pacific and the Bering Sea and reached the Arctic on 2 March. The geopotential height at 500 hPa showed that a high pressure stayed around the Bering Sea (200°E, 65°N) for more than five days from 27 February and a westerly jet split into two branches over the North Pacific: one toward the Bering Sea and the other toward North America. The poleward transport of East Asian BC was caused by the northward winds prevailing west of the blocking high. We found that the blocking anticyclone staying around the Bering Sea had an essential role in the Pacific route event. It took about five days for the East Asian BC to be transported from East Asia to the Arctic.

Previous studies indicated that long-range transport from East Asia to the Arctic occurs mainly in the middle troposphere and low-level transport is weak (Ikeda et al., 2017; Klonecki et al., 2003; Stohl, 2006). Di Pierro et al. (2011) reported that aerosol transports from East Asia to the Arctic took place at 3–7 km altitude and no plume was observed to reach the ground. While the model in this study demonstrated that enhancements of East Asian BC occurred in the middle troposphere (300–800 hPa) in many events (Figure 1), East Asian BC increased also in the lower troposphere for the event in March 2011 (Figures 1 and 3). Figure 4 shows the temporal variations of observed and simulated daily BC concentrations at Barrow, Alaska (156.6°W, 71.3°N). The observed BC showed an enhancement for 3–7 March, reaching a maximum of ~200 ng m^{-3} on 6 March. The model reproduced the observed BC increase at Barrow and indicated that this enhancement was mostly explained by East Asian BC (Figure 4). This result suggests that the enhancement of BC observed at Barrow was caused by downward transport of East Asian BC inflowed from the middle troposphere due to subsidence associated with the blocking high staying around the Bering Sea. The

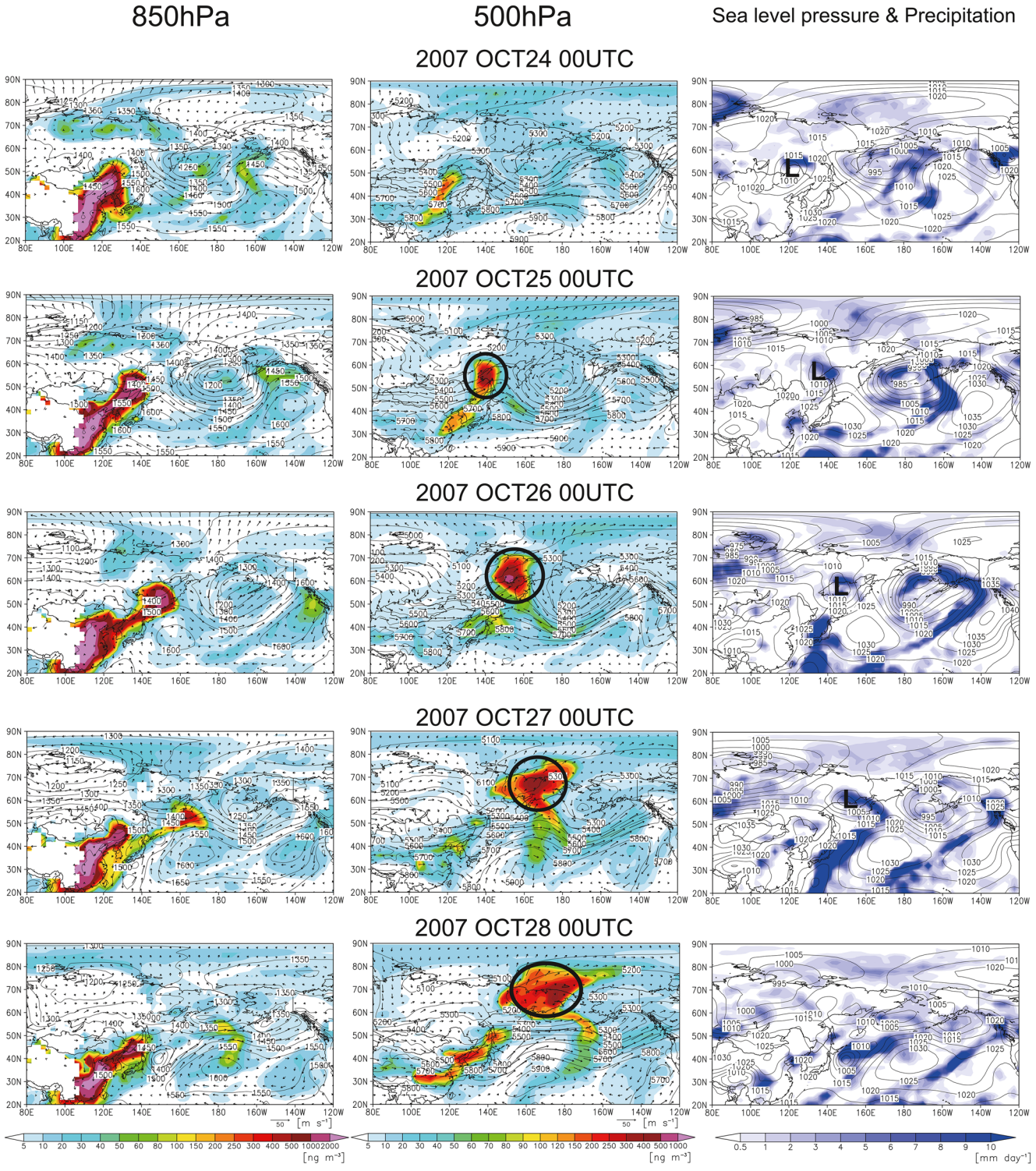

Figure 2. Left column: Simulated East Asian BC (color), geopotential height (solid line), and horizontal winds (arrow) at 850 hPa for October 24–28, 2007. Middle column: Same as the left column but for 500 hPa. Right column: Sea level pressure (solid line) and precipitation (color). Black circles indicate the plume of East Asian BC. L indicates the location of the low-pressure center.

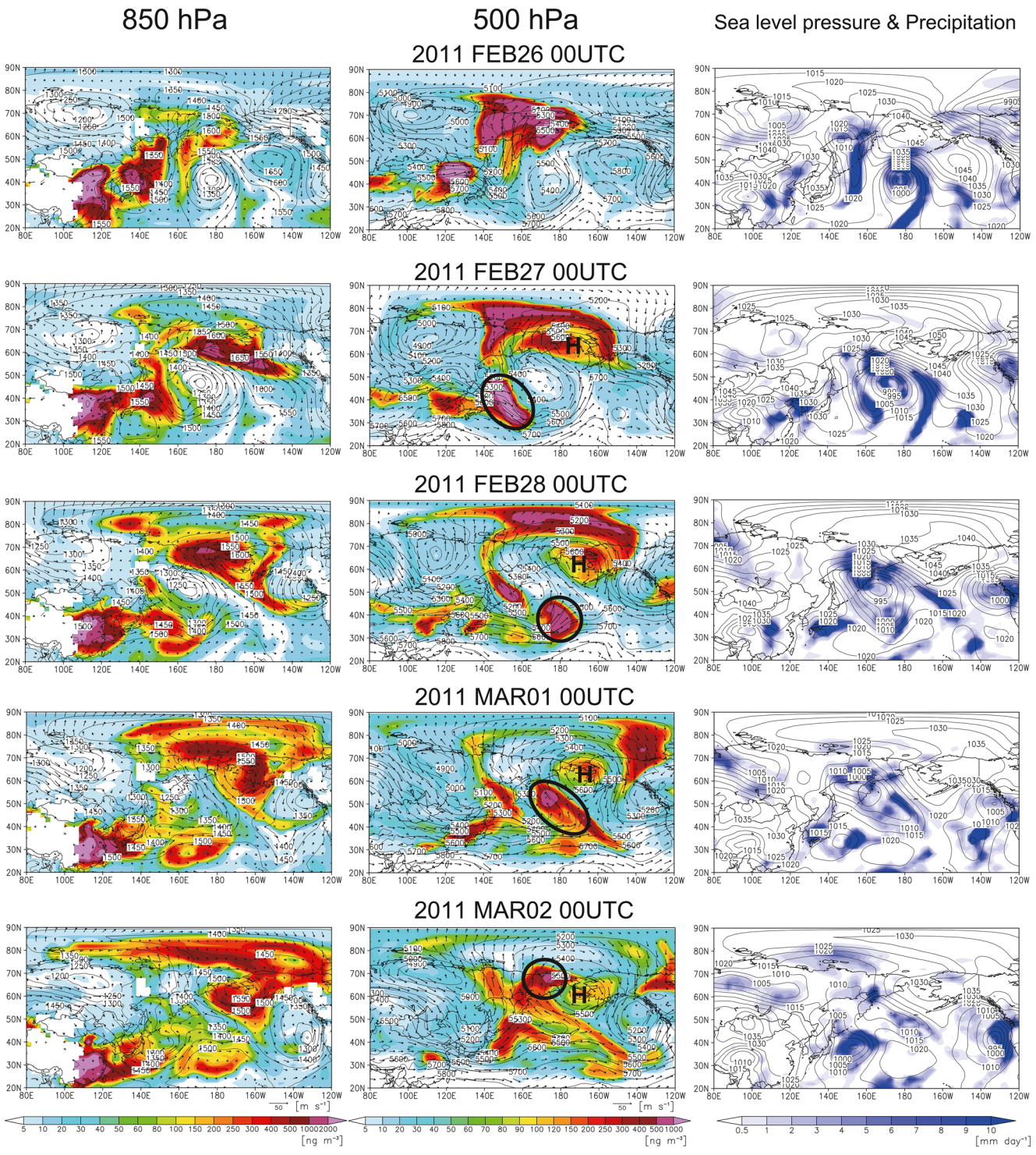

Figure 3. Left column: Simulated East Asian black carbon (BC) (color), geopotential height (solid line), and horizontal winds (arrow) at 850 hPa for February 26–March 2, 2011. Middle column: Same as the left column but for 500 hPa. Right column: Sea level pressure (solid line) and precipitation (color). Black circles indicate the plume of East Asian BC. H indicates the location of the high-pressure center.

downward transport to 850 hPa was seen around the Bering Sea from 27 February (Figure 3). The descending flow occurred on the eastern part of a high-pressure system around Alaska and the Bering Strait and caused the downward transport of East Asian BC to the lower troposphere (see also Figures S4 and S5). It means that East Asian BC can be transported in the lower troposphere including near the surface for events

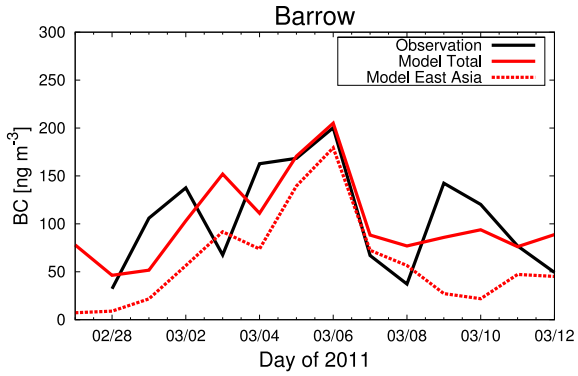

Figure 4. Temporal variations of observed and simulated daily mean black carbon (BC) concentrations at Barrow, Alaska. The black line indicates observations. Solid and dashed red lines show simulated total BC and East Asian BC, respectively.

of the Pacific route. Except for the event in March 2011, we could not confirm any increase in observed BC at Barrow due to long-range transport from East Asia during the events in 2007–2011.

We can distinguish two transport pathways from East Asia to the Arctic from the CO column measured by IASI. Figure 5 shows the horizontal distributions of the daily CO column for the events of the Siberian route in October 2007 and the Pacific route in February–March 2011. For the Siberia route, a high CO plume was transported from the Asian continent through the Sea of Okhotsk and East Siberia and reached the Arctic. This result is consistent with the transport pathway of East Asian BC demonstrated by the tagged simulation (Figure 2). For the Pacific route, the plume of CO was firstly transported eastward from East China to the North Pacific. After the export to the central North Pacific, it was transported poleward and reached the Arctic through the Bering Sea. This transport pattern is also consistent with that of the tagged BC simulation (Figure 3). Using IASI CO, we confirmed that there were two transport patterns from East Asia to the Arctic (see also Figure S6). We also compared CO columns simulated by GEOS-Chem with IASI CO and confirmed that the transport pathways of CO for these Siberian and Pacific route events were well reproduced by the model (see Figures S7 and S8).

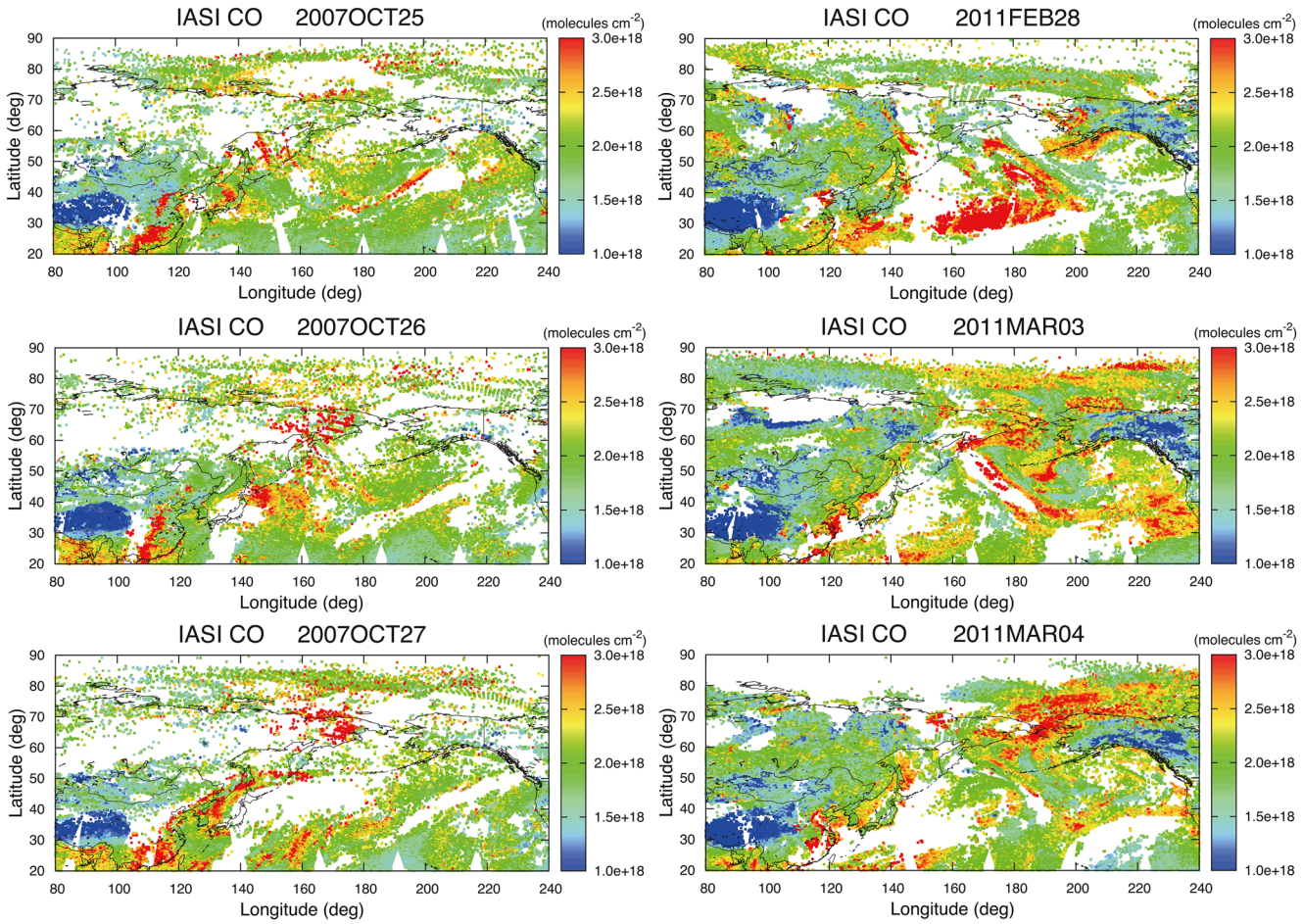

Figure 5. Horizontal distributions of daily CO column measured by IASI in October 2007 (left) and February–March 2011 (right).

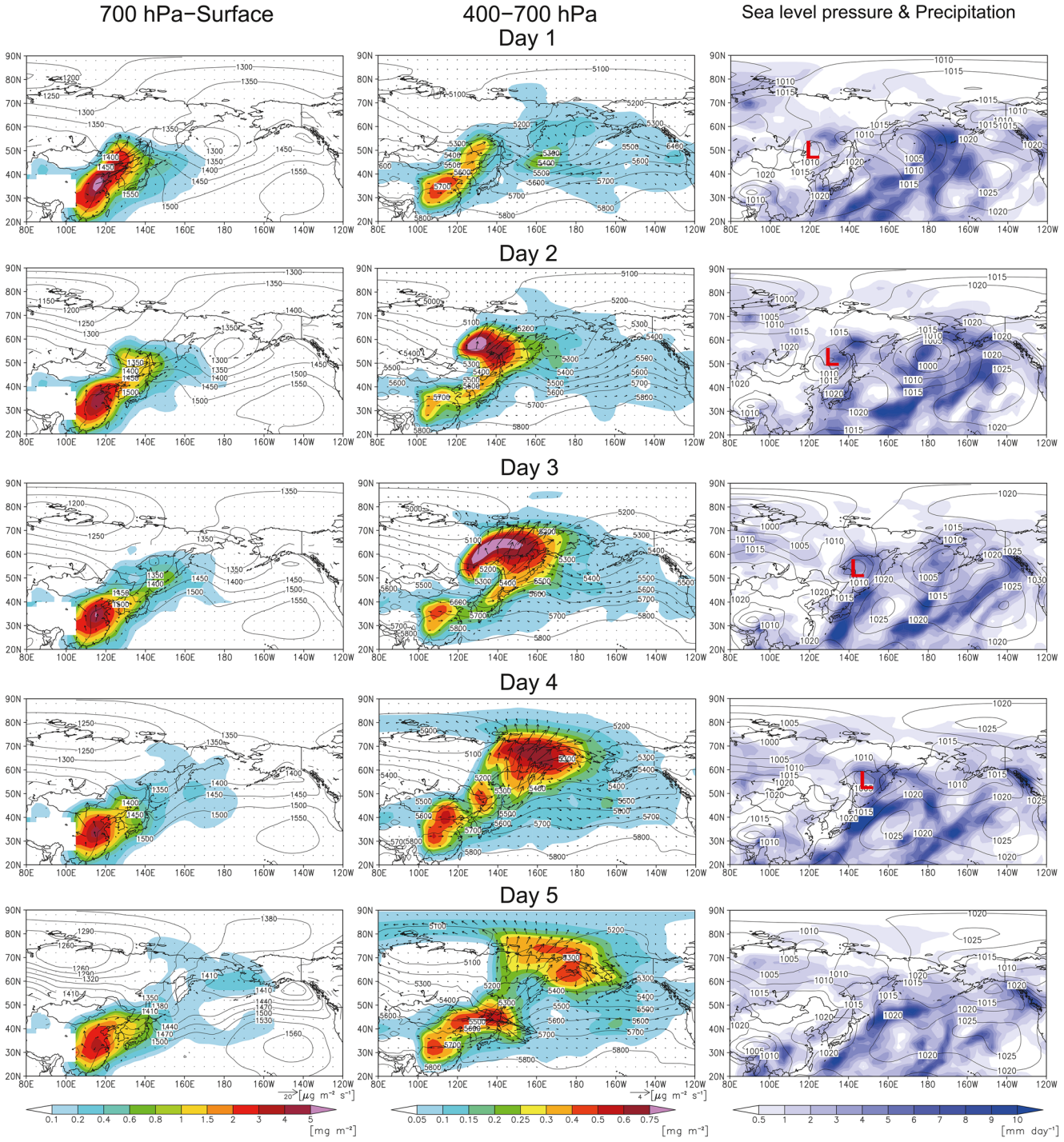

Figure 6. Composited black carbon (BC) column, horizontal BC fluxes, and geopotential height in the lower and middle troposphere for five events of the Siberian route. Sea level pressure and precipitation are also shown. L indicates the location of the low-pressure center.

3.4. Composite Analysis

To clarify the key features of the transport patterns and meteorological conditions of the Siberian route, a composite analysis was performed for six events. The composite was calculated by averaging the concentrations and the meteorological fields of the identified events. Figure 6 shows the composited column of East Asian BC in the lower (700 hPa–surface) and middle troposphere (400–700 hPa) for five days from the event

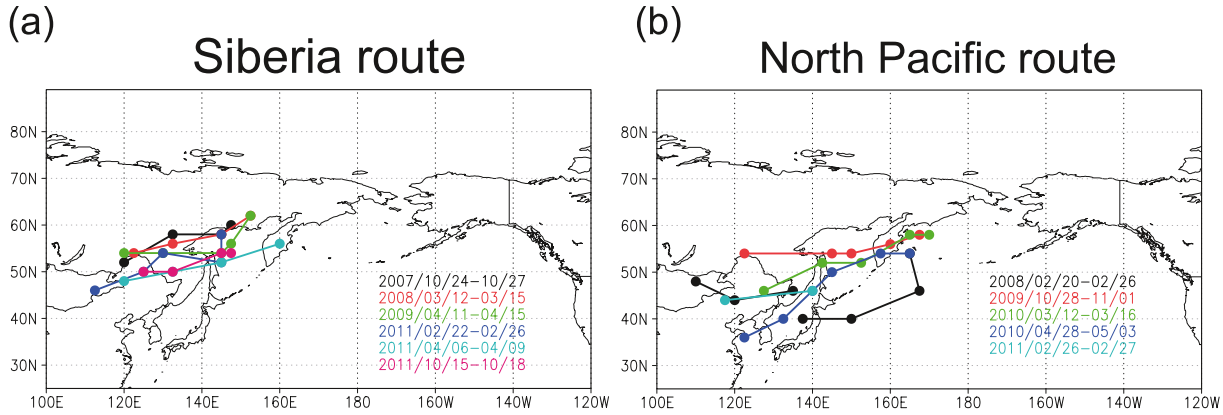

Figure 7. Cyclone tracks of individual events associated with (a) the Siberian route and (b) the Pacific route.

start to the arrival of BC at the Arctic. For the analysis of meteorological fields in the lower and middle troposphere, geopotential heights and horizontal winds at 850 hPa and 500 hPa were used, respectively. Figure 6 also shows the composited sea level pressure and precipitation. At an early stage, in the lower troposphere, a high BC band expanded northeastward from central eastern China to the Sea of Okhotsk. This transport was caused by northeastward winds blowing south of a low pressure at relatively high mid-latitude as described in the case study of October 2007. The composited sea level pressure showed that the averaged cyclone center moved northeastward from the border between China and Russia (120°E, 50°N) to the Sea of Okhotsk through East Siberia. Figure 7 shows the cyclone tracks of individual events of the Siberian route. We found that these low pressures had similar tracks moving northeastward from Northeast China or East Siberia to the Sea of Okhotsk.

From the BC column in the middle troposphere, we can see that upward transport to the free troposphere occurred over East Siberia (Day 2 in Figure 6). The uplifting took place around the low pressure, suggesting that a warm conveyor belt played an important role (Cooper et al., 2004). The high BC plume in the middle troposphere was transported northeastward and entered the Arctic three days after uplifting. The composited meteorological fields at 500 hPa showed that northeastward winds blew east of the trough and played an important role in the poleward transport of East Asian BC. This transport pathway was similar to the pathways reported by Di Pierro et al. (2011) that examined aerosol transport events from East Asia to the Arctic. They showed that aerosols originating from East Asia were transported through Siberia to the Arctic in the middle troposphere at 3–7 km altitudes. They also discussed the meteorological conditions associated with the transport events and pointed out that a high-pressure anomaly at 500 hPa in the Northwest Pacific was important to the poleward transport due to northward winds blowing west of this anomaly. This is basically consistent with the result of the present study showing that the poleward transport occurred between the trough and ridge.

Next, we examined the characteristics of the transport pattern of the Pacific route events using composites constructed in the same manner as those of the Siberian route (Figure 8). First, East Asian BC was transported eastward from East China to the North Pacific through Japan. The exports from the Asian continent were caused by low pressures that passed from North China or the East China Sea to the Bering Sea. In contrast to the Siberian route, the cyclones associated with the Pacific route events had various tracks (Figure 7). Some of the cyclone tracks of the Pacific route events were similar to those of the Siberian route events (October 2009 and March 2010). On the other hand, some cyclone tracks were seen south of 45°N at the early stage of the Pacific route events (February 2008, April 2010, and February 2011). Thus, a clear pattern of the low pressure was not seen in the composited sea level pressure at the early stage of the events (Figure 8). The variation in the cyclone tracks of the Pacific route events suggests that the existence of a blocking anticyclone around the Bering Sea is more important to these events than the cyclone tracks. The eastward transport from the Asian continent occurred at a lower latitude compared to that of the Siberian route. Over the North Pacific, the midlatitude westerly winds were interrupted by a blocking anticyclone staying around the Bering Sea, and a northward wind prevailed at 45–70°N, 150–180°E. The East Asian BC

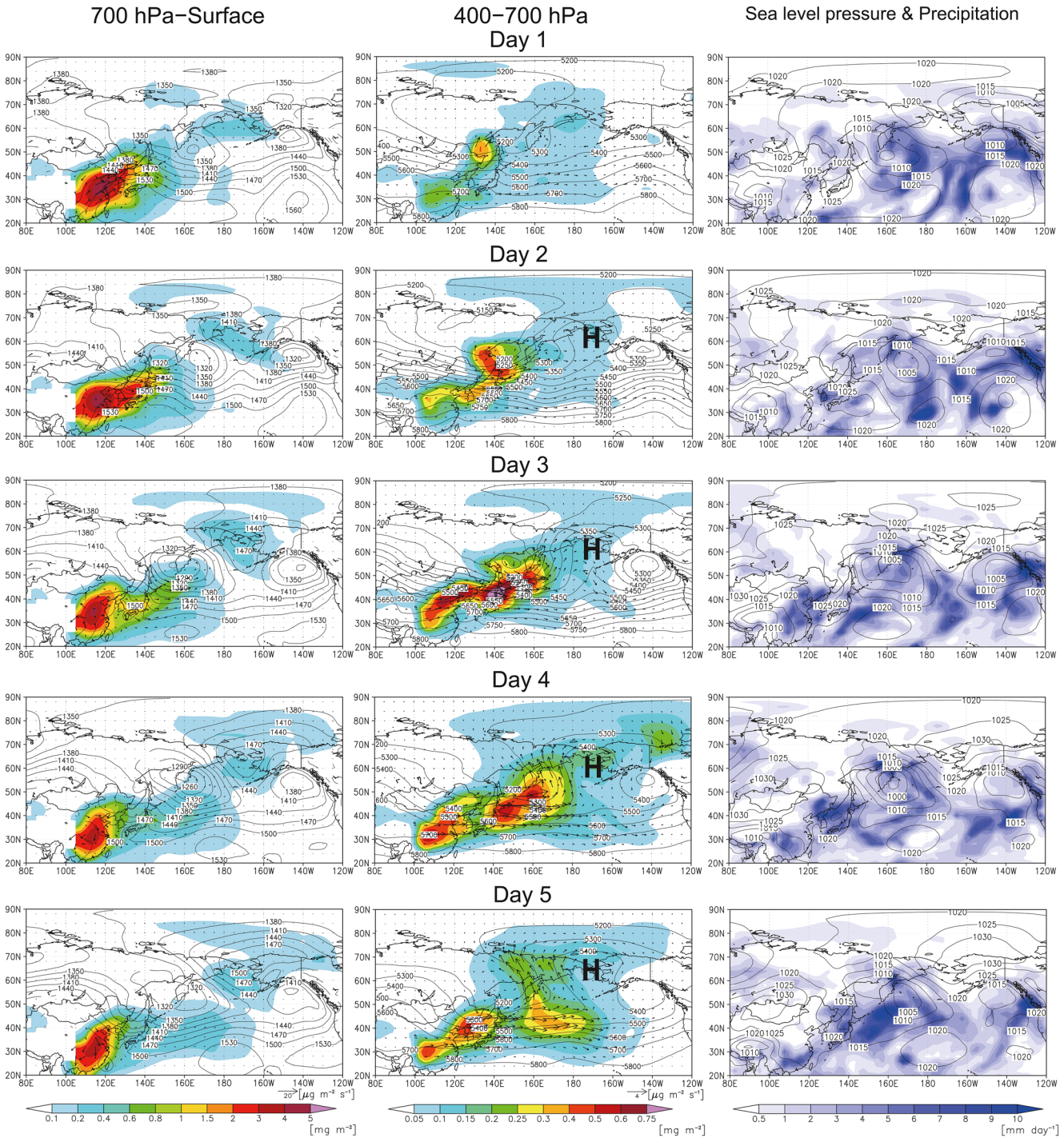

Figure 8. Composited black carbon (BC) column, horizontal BC fluxes, and geopotential height in the lower and middle troposphere for six events of the Pacific route. H indicates the location of the high-pressure center.

was transported northward by the southerly wind over the North Pacific and reached the Arctic through the Bering Sea. The anticyclone around the Bering Sea had an essential role in the poleward transport. The composited geopotential heights showed a clear blocking pattern, and northward winds continued to blow on the west side of this high pressure. The anticyclone was characterized by staying around the Bering Sea for at least five days during the events. The high pressure was seen not only in the middle troposphere but

also in the lower troposphere (850 hPa) and sea level pressure. The Bering Sea is one of the regions where blocking anticyclones most frequently occur in the Northern Hemisphere (Barriopedro et al., 2006).

The transport times from East Asia to the Arctic were 4–6 days and 5–7 days for the Siberian and the Pacific route events, respectively (Table 1). We estimated the transport times to the Arctic by tracking the plumes of East Asian BC based on the daily distributions. The transport patterns of the composite analysis for both pathways were similar to those of the case studies (Figures 2 and 3). The transport pathways of all 11 events are shown in the supporting information, indicating that other events for each pathway also had similar transport patterns (see Figure S3). The poleward transport was caused by northward winds blowing west of the high-pressure anomaly for both route events. However, while the synoptic disturbance moving northeastward over eastern Siberia played an important role in the Siberian route events, the blocking anticyclones staying around the Bering Sea caused northward transport for the Pacific route events. The East Asian BC was transported mainly in the middle troposphere into the Arctic. In the lower troposphere, the East Asian BC for the Pacific route was more widely distributed over the Arctic (>66°N) than that for the Siberian route. This is probably because the downward transport was caused by the high pressure staying around the Bering Sea as shown for the event in March 2011 when BC enhancement was observed even at the Arctic site. The Siberian route events occurred three times in spring, twice in autumn, and once in winter. On the other hand, the Pacific route events took place three times in spring, once in autumn, and once in winter. Thus, there is no clear difference in the season when the events of the two routes occurred during the period of 2007–2011.

4. Conclusions

We examined long-range transport events of BC and CO from East Asia to the Arctic during 2007–2011 to elucidate the transport mechanisms and meteorological conditions. Using the CO column measured by the IASI satellite, we identified 11 events that were defined by episodic enhancements over the Pacific Arctic (160–200°E, 60–80°N). These events occurred six times in spring, three times in autumn, and twice in winter. We investigated the transport patterns and meteorological fields of each event on a daily scale using tagged BC simulations with the global chemical transport model GEOS-Chem and found that there were two distinct transport pathways from East Asia to the Arctic: The Siberian route and the Pacific route. We also confirmed that these two transport patterns could be distinguished in the CO plumes measured by IASI.

For the Siberian route, BC originating from East Asia firstly spread northeastward from northern China to the Sea of Okhotsk in the lower troposphere. The East Asian BC uplifted to the middle troposphere was transported northeastward over eastern Siberia and reached the Arctic. A low pressure passing from northeast China to the Sea of Okhotsk played an important role throughout the event. For the Pacific route, the East Asian BC was exported to the Northwest Pacific through Japan, followed by a northward transport over the North Pacific and the Bering Sea. A blocking anticyclone that stayed around the Bering Sea and interrupted the westerlies played an essential role in the poleward transport because northward winds continued to blow west of this high pressure. During the event, BC enhancement was also observed at Barrow, suggesting that East Asian BC can be transported in the lower troposphere including near the surface for the Pacific route event. It has been reported that East Asian BC is transported to the Arctic mainly in the middle troposphere due to the uplifting during long-range transport. However, our result implies that East Asian BC can affect the Arctic climate due to deposition on snow and ice and reduce the surface albedo.

We then performed a composite analysis to clarify the key features of the transport patterns and the synoptic-scale meteorological fields of both route events. The composite also demonstrated the different transport pathways of the Siberian and Pacific routes. The composite sea level pressure for the Siberian route clearly showed a cyclone moving from northeast China to the Sea of Okhotsk. This is because the cyclones of the Siberian route events had similar tracks at relatively high mid-latitudes. The composite meteorological fields for the Pacific route showed a clear blocking high that stayed around the Bering Sea and interrupted the westerlies over the North Pacific. This anticyclone played a crucial role in the poleward transport of East Asian BC in the middle troposphere. Both the Siberian and Pacific route events most frequently took place

in spring, and thus there is no clear difference in the seasons when the events of the two routes occurred during the period of 2007–2011.

The findings in this study on the transport pathways and the associated meteorological conditions can provide valuable knowledge for the planning of field campaigns and model inter-comparison studies on long-range transport from East Asia to the Arctic. It was predicted that storm tracks in the extratropics would change in the future climate (e.g., Ulbrich et al., 2008), and thus these changes will affect long-range transport from East Asia to the Arctic. To examine the impact of the future climate on the transport from Asia to the Arctic, the transport processes indicated by the present study can be used as the characteristics of long-range transport from East Asia to the Arctic under the current climate. In future studies, it would be important to examine the transport of various air pollutants such as other aerosol species to the Arctic in addition to BC which was the main focus of this study.

Data Availability Statement

The model data is available from the NIES download site (https://fxp.nies.go.jp/public/7GFMQA7mIIvALA8BRmdzbDsiOnOUBTgk5J6stTqltnCr).

Acknowledgments
This research was supported by the Environmental Research and Technology Development Fund (2-1505 and 2-1803) of the Ministry of the Environment, Japan. IASI is a joint mission of Eumetsat and the Centre National d'Etudes Spatiales (CNES, France). The authors acknowledge the Aeris data infrastructure (https://www.aeris-data.fr/) for providing access to the IASI CO data used in this study. This work is a contribution to PACES (air Pollution in the Arctic: Climate Environment and Societies), an activity sponsored by the IGAC (International Global Atmospheric Chemistry) project.

References

AMAP (2015). *AMAP assessment 2015: Black carbon and ozone as Arctic climate forcers*. Oslo, Norway: Arctic monitoring and assessment programme (AMAP) (p. 116).

Arnold, S. R., Law, K. S., Brock, C. A., Thomas, J. L., Starkweather, S. M., von Salzen, K., et al. (2016). Arctic air pollution: Challenges and opportunities for the next decade. *Elementa: Science of the Anthropocene*, *4*, 000104. https://doi.org/10.12952/journal.elementa.000104

Barrie, L. A. (1986). Arctic air pollution: An overview of current knowledge. *Atmospheric Environment*, *20*, 643–663. https://doi.org/10.1016/0004-6981(86)90180-0

Barriopedro, D., García-Herrera, R., Lupo, A. R., & Hernández, E. (2006). A climatology of northern hemisphere blocking. *Journal of Climate*, *19*(6), 1042–1063. https://doi.org/10.1175/jcli3678.1

Bey, I., Jacob, D. J., Logan, J. A., & Yantosca, R. M. (2001). Asian chemical outflow to the Pacific in spring: Origins, pathways, and budgets. *Journal of Geophysical Research*, *106*, 23097–23113. https://doi.org/10.1029/2001jd000806

Bourgeois, Q., & Bey, I. (2011). Pollution transport efficiency toward the Arctic: Sensitivity to aerosol scavenging and source regions. *Journal of Geophysical Research*, *116*, D08213. https://doi.org/10.1029/2010jd015096

Chen, S.-J., Kuo, Y.-H., Zhang, P.-Z., & Bai, Q.-F. (1991). Synoptic climatology of cyclogenesis over East Asia, 1958-1987. *Monthly Weather Review*, *119*, 1407. https://doi.org/10.1175/1520-0493(1991)119<1407:scocoe>2.0.co;2

Clarisse, L., Fromm, M., Ngadi, Y., Emmons, L., Clerbaux, C., Hurtmans, D., et al. (2011). Intercontinental transport of anthropogenic sulfur dioxide and other pollutants: An infrared remote sensing case study. *Geophysical Research Letters*, *38*, L19806. https://doi.org/10.1029/2011gl048976

Clerbaux, C., Boynard, A., Clarisse, L., George, M., Hadji-Lazaro, J., Herbin, H., et al. (2009). Monitoring of atmospheric composition using the thermal infrared IASI/MetOp sounder. *Atmospheric Chemistry and Physics*, *9*, 6401–6054. https://doi.org/10.5194/acp-9-6041-2009

Cooper, O. R., Forster, C., Parrish, D., Trainer, M., Dunlea, E., Ryerson, T., et al. (2004). A case study of transpacific warm conveyor belt transport: Influence of merging airstreams on trace gas import to North America. *Journal of Geophysical Research*, *109*, D23S08. https://doi.org/10.1029/2003jd003624

Di Pierro, M., Jaeglé, L., & Anderson, T. L. (2011). Satellite observations of aerosol transport from East Asia to the Arctic: Three case studies. *Atmospheric Chemistry and Physics*, *11*, 2225–2243. https://doi.org/10.5194/acp-11-2225-2011

Eckhardt, S., Quennehen, B., Olivié, D. J. L., Berntsen, T. K., Cherian, R., Christensen, J. H., et al. (2015). Current model capabilities for simulating black carbon and sulfate concentrations in the Arctic atmosphere: A multi-model evaluation using a comprehensive measurement data set. *Atmospheric Chemistry and Physics*, *15*, 9413–9433. https://doi.org/10.5194/acp-15-9413-2015

Flanner, M. G., Zender, C. S., Randerson, J. T., & Rasch, P. J. (2007). Present-day climate forcing and response from black carbon in snow. *Journal of Geophysical Research*, *112*, D11202. https://doi.org/10.1029/2006jd008003

George, M., Clerbaux, C., Hurtmans, D., Turquety, S., Coheur, P.-F., Pommier, M., et al. (2009). Carbon monoxide distributions from the IASI/METOP mission: evaluation with other space-borne remote sensors. *Atmospheric Chemistry and Physics*, *9*, 8317–8330. https://doi.org/10.5194/acp-9-8317-2009

Hadley, O. L., Ramanathan, V., Carmichael, G. R., Tang, Y., Corrigan, C. E., Roberts, G. C., & Mauger, G. S. (2007). Trans-Pacific transport of black carbon and fine aerosols ($D < 2.5\ \mu$m) into North America. *Journal of Geophysical Research*, *112*, D05309. https://doi.org/10.1029/2006jd007632

Hirdman, D., Sodemann, H., Eckhardt, S., Burkhart, J. F., Jefferson, A., Mefford, T., et al. (2010). Source identification of short-lived air pollutants in the Arctic using statistical analysis of measurement data and particle dispersion model output. *Atmospheric Chemistry and Physics*, *10*, 669–693. https://doi.org/10.5194/acp-10-669-2010

Ikeda, K., Tanimoto, H., Sugita, T., Akiyoshi, H., Kanaya, Y., Zhu, C., & Taketani, F. (2017). Tagged tracer simulations of black carbon in the Arctic: Transport, source contributions, and budget. *Atmospheric Chemistry and Physics*, *17*, 10515–10533. https://doi.org/10.5194/acp-17-10515-2017

Janssens-Maenhout, G., Crippa, M., Guizzardi, D., Dentener, F., Muntean, M., Pouliot, G., et al. (2015). HTAP_v2.2: A mosaic of regional and global emission grid maps for 2008 and 2010 to study hemispheric transport of air pollution. *Atmospheric Chemistry and Physics*, *15*, 11411–11432. https://doi.org/10.5194/acp-15-11411-2015

Klonecki, A., Hess, P., Emmons, L., Smith, L., Orlando, J., & Blake, D. (2003). Seasonal changes in the transport of pollutants into the Arctic troposphere-model study. *Journal of Geophysical Research*, *108*(D4), 8367. https://doi.org/10.1029/2002jd002199

Lee, Y. H., Lamarque, J.-F., Flanner, M. G., Jiao, C., Shindell, D. T., Berntsen, T., et al. (2013). Evaluation of preindustrial to present-day black carbon and its albedo forcing from Atmospheric chemistry and climate model intercomparison project (ACCMIP). *Atmospheric Chemistry and Physics*, *13*, 2607–2634. https://doi.org/10.5194/acp-13-2607-2013

Liang, Q., Jaeglé, L., Jaffe, D. A., Weiss-Penzias, P., Heckman, A., & Snow, J. A. (2004). Long-range transport of Asian pollution to the northeast Pacific: Seasonal variations and transport pathways of carbon monoxide. *Journal of Geophysical Research*, *109*, D23S07. https://doi.org/10.1029/2003jd004402

Liu, J., Fan, S., Horowitz, L. W., & Levy, H., II (2011). Evaluation of factors controlling long-range transport of black carbon to the Arctic. *Journal of Geophysical Research*, *116*, D00A14. https://doi.org/10.1029/2010jd015145

Luan, Y., & Jaeglé, L. (2013). Composite study of aerosol export events from East Asia and North America. *Atmospheric Chemistry and Physics*, *13*, 1221–1242. https://doi.org/10.5194/acp-13-1221-2013

Lund, M. T., Samset, B. H., Skeie, R. B., Watson-Parris, D., Katich, J. M., Schwarz, J. P., et al. (2018). Short black carbon lifetime inferred from a global set of aircraft observations. *npj Climate and Atmospheric Science*, *1*, 31. https://doi.org/10.1038/s41612-018-0040-x

Matsui, H., Kondo, Y., Moteki, N., Takegawa, N., Sahu, L. K., Zhao, Y., et al. (2011). Seasonal variation of the transport of black carbon aerosol from the Asian continent to the Arctic during the ARCTAS aircraft campaign. *Journal of Geophysical Research*, *116*, D05202. https://doi.org/10.1029/2010jd015067

Oshima, N., Koike, M., Kondo, Y., Nakamura, H., Moteki, N., Matsui, H., et al. (2013). Vertical transport mechanisms of black carbon over East Asia in spring during the A-FORCE aircraft campaign. *Journal of Geophysical Research: Atmospheres*, *118*, 13175–13198. https://doi.org/10.1002/2013jd020262

Quinn, P. K., Bates, T. S., Baum, E., Doubleday, N., Fiore, A. M., Flanner, M., et al. (2008). Short-lived pollutants in the Arctic: Their climate impact and possible mitigation strategies. *Atmospheric Chemistry and Physics*, *8*, 1723–1735. https://doi.org/10.5194/acp-8-1723-2008

Quinn, P. K., Shaw, G., Andrews, E., Dutton, E. G., Ruoho-Airola, T., & Gong, S. L. (2007). Arctic haze: Current trends and knowledge gaps. *Tellus B: Chemical and Physical Meteorology*, *59*, 99–114. https://doi.org/10.1111/j.1600-0889.2006.00236.x

Sand, M., Berntsen, T. K., von Salzen, K., Flanner, M. G., Langner, J., & Victor, D. G. (2016). Response of Arctic temperature to changes in emissions of short-lived climate forcers. *Nature Climate Change*, *6*, 286–289. https://doi.org/10.1038/nclimate2880

Sharma, S., Ishizawa, M., Chan, D., Lavoué, D., Andrews, E., Eleftheriadis, K., & Maksyutov, S. (2013). 16-year simulation of Arctic black carbon: Transport, source contribution, and sensitivity analysis on deposition. *Journal of Geophysical Research: Atmospheres*, *118*, 943–964. https://doi.org/10.1029/2012jd017774

Shindell, D. (2007). Local and remote contributions to Arctic warming. *Geophysical Research Letters*, *34*, L14704. https://doi.org/10.1029/2007gl030221

Shindell, D. T., Chin, M., Dentener, F., Doherty, R. M., Faluvegi, G., Fiore, A. M., et al. (2008). A multi-model assessment of pollution transport to the Arctic. *Atmospheric Chemistry and Physics*, *8*, 5353–5372. https://doi.org/10.5194/acp-8-5353-2008

Stohl, A. (2006). Characteristics of atmospheric transport into the Arctic troposphere. *Journal of Geophysical Research*, *111*, D11306. https://doi.org/10.1029/2005jd006888

Stohl, A., Andrews, E., Burkhart, J. F., Forster, C., Herber, A., Hoch, S. W., et al. (2006). Pan-Arctic enhancements of light absorbing aerosol concentrations due to North American boreal forest fires during summer 2004. *Journal of Geophysical Research*, *111*, D22214. https://doi.org/10.1029/2006jd007216

Ulbrich, U., Pinto, J. G., Kupfer, H., Leckebusch, G. C., Spangehl, T., & Reyers, M. (2008). Changing Northern Hemisphere storm tracks in an ensemble of IPCC climate change simulations. *Journal of Climate*, *21*, 1669–1679. https://doi.org/10.1175/2007jcli1992.1

van der Werf, G. R., Randerson, J. T., Giglio, L., Collatz, G. J., Mu, M., Kasibhatla, P. S., et al. (2010). Global fire emissions and the contribution of deforestation, savanna, forest, agricultural, and peat fires (1997-2009). *Atmospheric Chemistry and Physics*, *10*, 11707–11735. https://doi.org/10.5194/acp-10-11707-2010

Wang, H. L., Rasch, P. J., Easter, R. C., Singh, B., Zhang, R. D., Ma, P. L., et al. (2014). Using an explicit emission tagging method in global modeling of source-receptor relationships for black carbon in the Arctic: Variations, sources, and transport pathways. *Journal of Geophysical Research: Atmospheres*, *119*, 12888–12909. https://doi.org/10.1002/2014jd022297

Wang, Q., Jacob, D. J., Fisher, J. A., Mao, J., Leibensperger, E. M., Carouge, C. C., et al. (2011). Sources of carbonaceous aerosols and deposited black carbon in the Arctic in winter-spring: Implications for radiative forcing. *Atmospheric Chemistry and Physics*, *11*, 12453–12473. https://doi.org/10.5194/acp-11-12453-2011

Reference From the Supporting Information

Rolph, G., Stein, A., & Stunder, B. (2017). Real-time environmental applications and display system: READY. *Environmental Modelling & Software*, *95*, 210–228. https://doi.org/10.1016/j.envsoft.2017.06.025